◆ Making Smart Use of Excess Antennas: Massive MIMO, Small Cells, and TDD

Jakob Hoydis, Kianoush Hosseini, Stephan ten Brink, and Mérouane Debbah

In this paper, we present a vision beyond the conventional Long Term Evolution Fourth Generation (LTE-4G) evolution path and suggest that time division duplexing (TDD) could be a key enabler for a new heterogeneous network architecture with the potential to provide ubiquitous coverage and unprecedented spectral area efficiencies. This architecture is based on a co-channel deployment of macro base stations (BSs) with very large antenna arrays and a secondary tier of small cells (SCs) with a few antennas each. Both tiers employ a TDD protocol in a synchronized fashion. The resulting channel reciprocity enables not only the estimation of large-dimensional channels at the BSs, but also an implicit coordination between both tiers without the need to exchange user data or channel state information (CSI) over the backhaul. In particular, during the uplink (UL), the BSs and SCs can locally estimate the dominant interference sub-space. This knowledge can be leveraged for downlink (DL) precoding to reduce intra- and inter-tier interference. In other words, the BSs and SCs "sacrifice" some of their degrees of freedom for interference rejection. Our simulation results demonstrate that the proposed architecture and precoding scheme can achieve a very attractive rate region compared to several baseline scenarios. For example, with 100 antennas at each BS and four antennas at each SC, we observe an aggregate area throughput of 7.63 Gb/s/km^2 (DL) and 8.93 Gb/s/km^2 (UL) on a 20 MHz band shared by about 100 mobile devices. © 2013 Alcatel-Lucent.

Introduction

The biggest challenge in the wireless industry today is to support the ever-growing demands for higher data rates and to ensure a consistent quality of service (QoS) throughout the entire network. Rising to this challenge means increasing network capacity by a factor of thousand over the next ten years [28]. Since spectral resources are scarce, there is a broad consensus that this can only be achieved by a massive network densification, i.e., a significant increase in the number of antennas deployed per unit area. In general, there are two approaches for this. The first approach relies on using more antennas at the existing cell sites to spatially multiplex user equipment

Bell Labs Technical Journal 18(2), 5–21 (2013) © 2013 Alcatel-Lucent. Published by Wiley Periodicals, Inc.
Published online in Wiley Online Library (wileyonlinelibrary.com) • DOI: 10.1002/bltj.21602

(UEs) on the same time-frequency resource. Once the number of antennas largely exceeds the number of actively transmitting or receiving UEs per cell, we are speaking about large-scale or "massive" multiple input multiple output (MIMO) systems [23]. The second approach is based on a dense deployment of small cells (SCs) which also increases the spatial reuse since less UEs share the resources of a single cell [5, 15]. Thus, cellular networks are going to be operated in a regime where the number of serving antennas equals or exceeds the number of UEs. As antennas become a commodity, it is natural to ask how the new abundance of degrees of freedom can be exploited efficiently.

Although the benefits of using multiple antennas at a transmitter and/or a receiver are well studied [10, 34], it was revealed only recently that very large antenna arrays can provide tremendous performance gains [23, 31]. Massive MIMO cannot only allow for aggressive spatial multiplexing and improved link reliability, but can also reduce the radiated power due to significant array gains [25]. Since such antenna arrays are composed of cheap low-power components, which can be integrated in existing cell sites or buildings (facades, windows, and other deployments), they could revolutionize the way traditional base stations (BSs) are built and deployed. However, in order to reap the benefits of a large number of coordinated antennas, channel state information (CSI) must be available at the transmitter. For this reason, massive MIMO systems find their sweet spot in the time division duplexing (TDD) mode where channel reciprocity can be exploited. This allows a BS to estimate its downlink (DL) channels from uplink (UL) pilots sent by the UEs. Therefore, the resulting overhead scales linearly with the number of UEs and is independent of the number of antennas [23]. The authors in [3] argue that the performance gains of massive MIMO can also be realized in frequency division duplexing (FDD) systems, given that certain assumptions about the antenna correlation hold true and that information about the channel covariance matrix is available at the transmitter. Nevertheless, since massive MIMO suffers from some practical limitations, such as pilot contamination [19] and antenna correlation [26], it is unlikely that this type of network densification alone can satisfy future traffic demands.

Panel 1. Abbreviations, Acronyms, and Terms

4G—Fourth generation
BS—Base station
coRTDD—Co-channel reverse TDD
coTDD—Co-channel TDD
CSI—Channel state information
DL—Downlink
FDD—Frequency division duplex
GPS—Global Positioning System
LOS—Line-of-sight
LTE—Long Term Evolution
MIMO—Multiple input multiple output
MMSE—Minimum mean square error
MUE—Macro user equipment
NLOS—Non line-of-sight
QoS—Quality of service
RF—Radio frequency
RTDD—Reverse time division duplex
SC—Small cell
SINR—Signal-to-interference-plus-noise ratio
SUE—Small cell user equipment
TDD—Time division duplex
UE—User equipment
UL—Uplink

On a separate track, shrinking the size of cells has been the single most effective way to increase network capacity [36]. This is because the capacity scales, at least in theory, linearly with the cell density. Moreover, the total transmit power of the network could be reduced since the cell density is proportional to the square of the cell radius while the path loss is proportional to the distance raised by some path loss exponent which is typically greater than two [16]. Thus, the capacity improvement does not come at the cost of an increase in the radiated energy [30]. Nevertheless, regardless of the difficulties and costs related to cell site acquisition, backhaul provision, and operation, deploying a large number of SCs can possibly exacerbate network performance. In particular, with antennas located below the rooftops and cell radii of less than 50 meters, supporting highly mobile UEs and providing seamless coverage over large areas

become increasingly difficult. Hence, SCs alone are unlikely to meet QoS and capacity requirements for next-generation mobile networks. A simple solution to this problem is a two-tier network architecture, where macro BSs ensure outdoor coverage and serve highly mobile UEs, while SCs act as the main capacity-driver for indoor and outdoor hotspots. However, with limited spectral resources, a co-channel deployment of BSs and SCs is the only viable solution, and this in turn calls for low-complexity and distributed interference management schemes across both tiers [7, 29, 37]. A well-known technique for time-domain interference cancellation is the use of "almost blank subframes" which are under consideration for the Long Term Evolution (LTE) Advanced standard [1].

In this paper, we present a TDD-based network architecture consisting of a massive MIMO macro tier overlaid with a second tier of SCs. Our goal is to integrate the complementary benefits of both. The key observation is that the synchronized operation of a TDD protocol in both tiers results in a channel reciprocity which facilitates not only the estimation of large-dimensional channels at the BSs, but also enables all devices in the network (BSs, SCs, UEs) to learn the eigenstructure of their interfering channels with no additional overhead. This information can be leveraged to design precoders which trade off beamforming gains against a reduction of interference imposed on the rest of the network. In other words, the SCs and BSs sacrifice some of their degrees of freedom (or "excess antennas") to reduce intra- and inter-tier interference. This enables some form of implicit cooperation between all devices in the network which does not necessitate any form of data or CSI exchange. Moreover, this scheme is fully distributed, easily scalable, and realizes the additional benefits of TDD, such as reduced latency, the ability to operate in unpaired frequency bands, and the support of asymmetric traffic [4]. We also consider a variant of the TDD protocol, called reverse TDD (RTDD). In contrast to TDD, the order of the UL and DL periods in one of the tiers is reversed, i.e., while the macro BSs are in the DL mode, the SCs are in the UL mode and vice versa. The choice of the duplexing mode determines which nodes of each tier interfere with each other. Hence, depending on the network topology, RTDD may or may not outperform TDD. Our simulation results show that a co-channel deployment of SCs and massive MIMO BSs in conjunction with either TDD or RTDD and the proposed precoding scheme leads to a very promising rate region compared to some baseline scenarios. In particular, we observe an aggregate area throughput of 7.63 Gb/s/km^2 (DL) and 8.93 Gb/s/km^2 (UL) on a 20 MHz band shared by about 100 UEs. This rate could be easily increased by increasing the bandwidth, installing more antennas at the BSs, or adding more SCs.

Related Work

The precoding design problem using interference covariance knowledge has been extensively studied in cognitive radio networks. In this context, a secondary transmitter acquires useful information about the interfering links in order to minimize interference imposed on a primary transmitter-receiver pair [38]. A similar approach is proposed in [22] in order to maximize the sum rate in a two-cell TDD system. However, our extension of this concept to dense heterogeneous networks operating a TDD-protocol in a synchronized fashion is new. RTDD or time-shifted TDD protocols have been previously proposed to reduce the negative effects of pilot contamination in TDD cellular systems [9]. RTDD is also considered in [2], where, building upon the UL-DL duality established in [24], a distributed power allocation algorithm is proposed to ensure symmetric UL-DL rates in both tiers. However, this scheme is based on a distributed iterative power allocation algorithm which needs to run over multiple channel coherence blocks to converge.

The remainder of this paper is structured as follows. In the next section, we present a general system model, explain different duplexing schemes, and discuss our proposed precoding technique. We then present some numerical results and evaluate the performance in an outdoor deployment scenario. Next, we discuss practical issues such as channel reciprocity and channel estimation and outline possible extensions. We finish with a summary and conclusions.

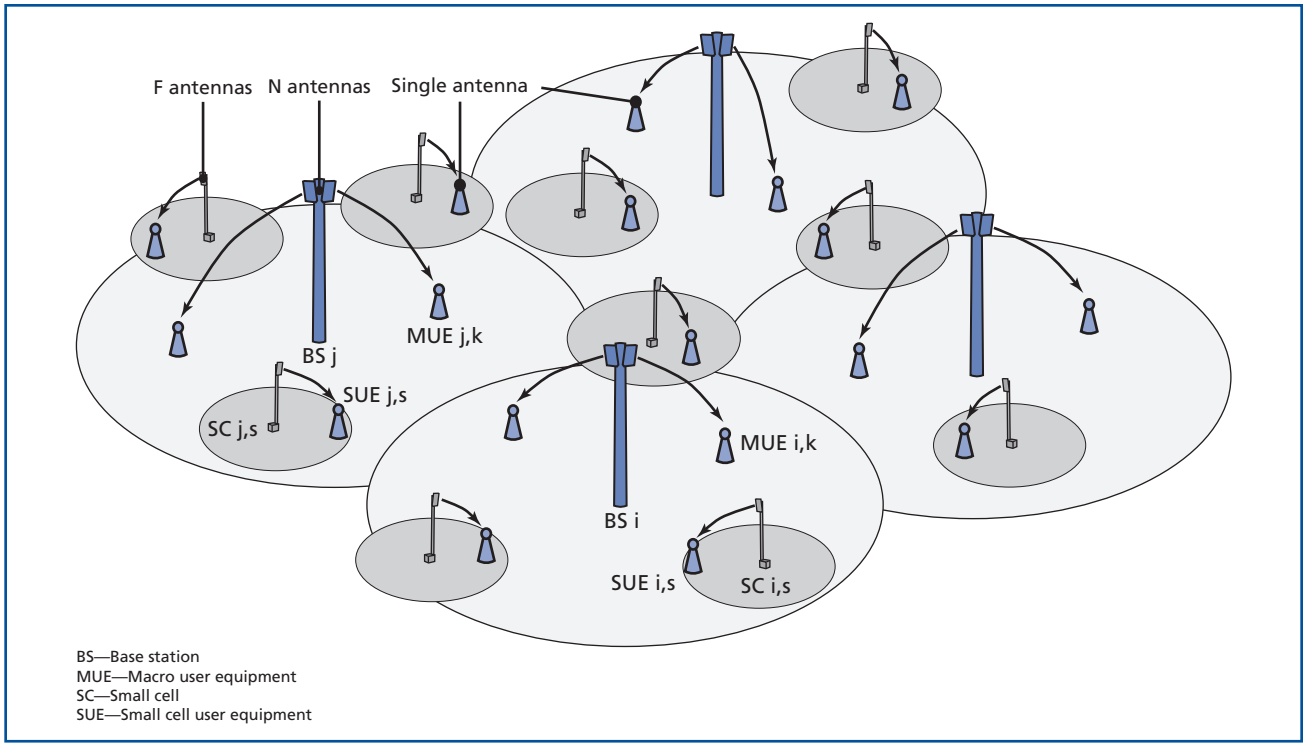

Figure 1.
Example of a two-tier network architecture. A macro-cell tier is overlaid with a dense tier of small cells.

System Model and Precoding Scheme

We consider a two-tier network consisting of B macro BSs wherein each cell is overlaid with a dense tier of S SCs, as exemplarily shown in **Figure 1**. The BSs and SCs are respectively equipped with N and F antennas. Each BS serves $K \leq N$ macro UEs (MUEs) while each SC serves a single small cell UE (SUE). The MUEs and SUEs have only one antenna. Extensions to multi-antenna UEs and multiple SUEs per SC are straightforward, but not considered here for clarity of presentation. Generally, F would lie somewhere in the range from 1 to 4 (as is state-of-the-art for Wi-Fi access points [18]), while N could be very large, i.e., 100, 1000, or even more [31].

In this setting, we compare the performance of four different duplexing modes, namely:

- Frequency division duplexing (FDD),
- Time division duplexing (TDD),
- Co-channel TDD (coTDD), and
- Co-channel reverse TDD (coRTDD).

The operating principles for each are illustrated in **Figure 2**. In both the FDD and TDD schemes, the BS and SC tiers operate on non-overlapping frequency bands, while UL and DL transmissions are duplexed in either frequency (FDD) or time (TDD). Although transmissions do not interfere across the tiers, the main performance-limiting factor is intra-tier interference which is particularly severe among the SCs. Unlike the aforementioned schemes, with coTDD and coRTDD, both tiers share the entire bandwidth. While the UL and DL transmissions are synchronized in both tiers with coTDD, their order is reversed in one of the tiers with coRTDD, i.e., the BSs are in DL mode while the SCs operate in UL mode, and vice versa. The duplexing mode determines which groups of devices interfere with each other. For example, in coTDD, the SUEs interfere with the MUEs in the UL while the BSs interfere with the SCs in the DL. This behavior is shown in **Figure 3**. Note that we assume perfect synchronization across all devices in the

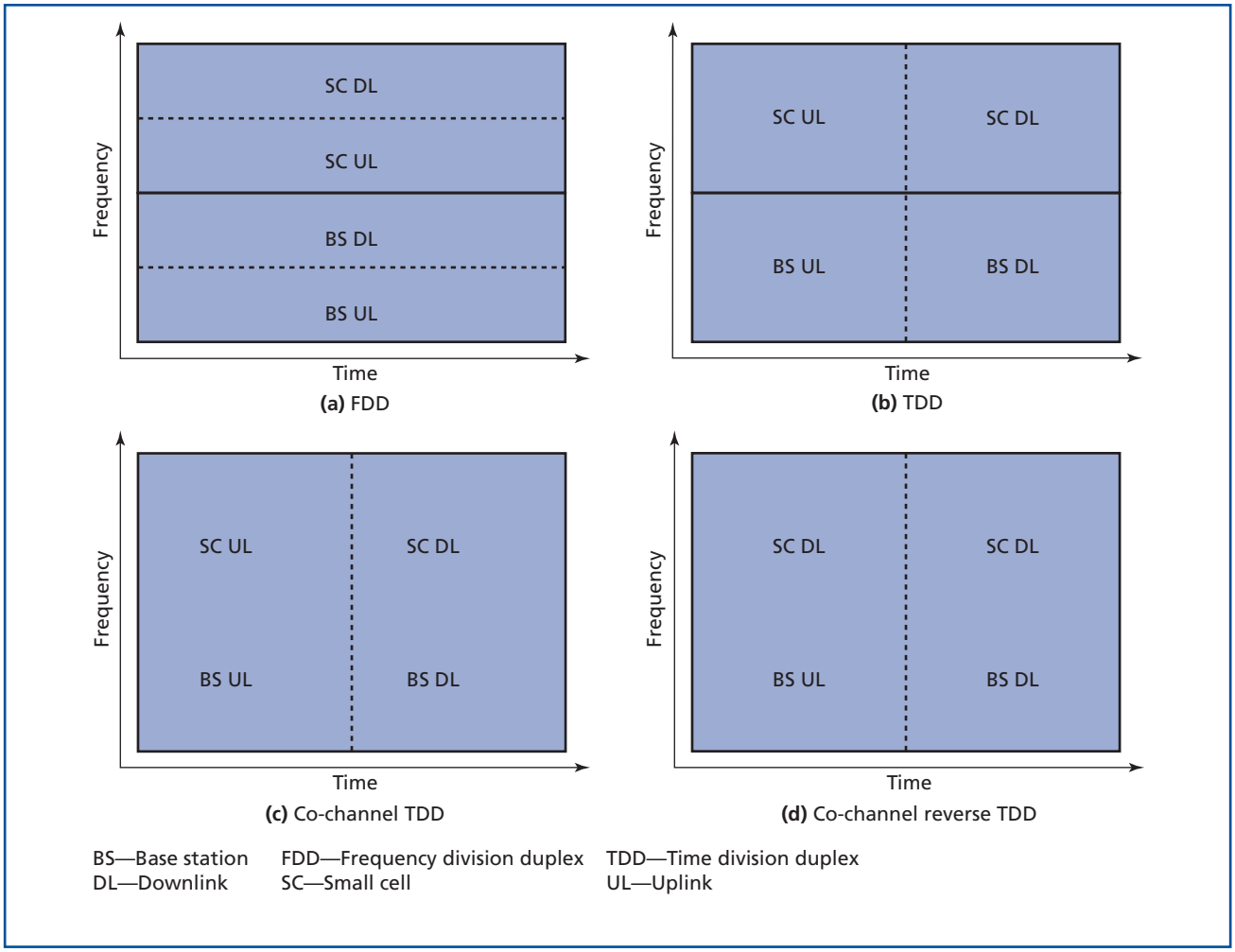

Figure 2.
Operating principles of different duplexing schemes.

network. Without loss of generality, we consider a frequency-flat block-fading channel model with coherence time T. Additionally, we make the simplifying assumption that the association of UEs to BSs or SCs has already been carried out. Our performance metric is the UL/DL sum rate of both tiers without any form of power control, scheduling, and consideration of fairness. Perfect CSI of the local channels at all devices in the network is assumed. Later in the paper, we further discuss the implications of some of these assumptions. The next section will present the detailed signaling model for the coTDD scheme. Since the TDD, FDD, and coRTDD schemes are very similar, they will only be briefly summarized in the section titled "Other Duplexing Schemes."

Co-Channel TDD Uplink

The received UL baseband signal vectors at BS i and SC j in cell i at time t are respectively given as

$$y_i^{BS}(t) = \sum_{b=1}^{B} \left(\sum_{k=1}^{K} \sqrt{P_{MUE}}\, h_{ibk}^{BS-MUE}\, x_{bk}^{MUE}(t) + \sum_{s=1}^{S} \sqrt{P_{SUE}}\, h_{ibs}^{BS-SUE}\, x_{bs}^{SUE}(t) \right) + n_i^{BS}(t) \quad (1)$$

$$y_{ij}^{SC}(t) = \sum_{b=1}^{B} \left(\sum_{k=1}^{K} \sqrt{P_{MUE}}\, h_{ijbk}^{SC-MUE}\, x_{bk}^{MUE}(t) + \sum_{s=1}^{S} \sqrt{P_{SUE}}\, h_{ijbs}^{SC-SUE}\, x_{bs}^{SUE}(t) \right) + n_{ij}^{SC}(t) \quad (2)$$

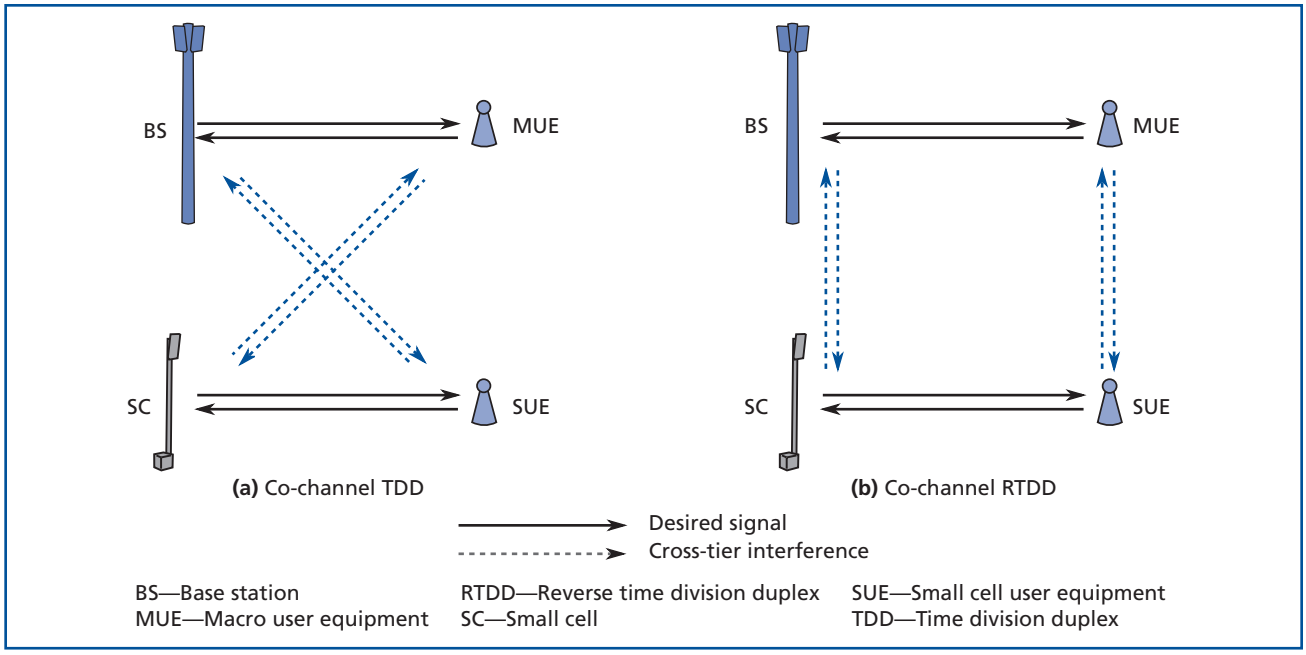

Figure 3.
Interfering links in co-channel TDD and RTDD.

where $x_{bk}^{MUE}(t)$ and $x_{bs}^{SUE}(t)$ are the complex Gaussian transmitted data symbols from the kth MUE and the sth SUE in cell b, h_{ibk}^{BS-MUE} and h_{ijbk}^{SC-MUE} denote the channel vectors from the kth MUE in cell b to the ith BS and the jth SC in cell i, $h_{ibs}^{BS-SUE}$and h_{ijbs}^{SC-SUE} denote the channel vectors from the sth SUE in cell b to the ith BS and the jth SC in cell i, and $n_i^{BS}(t)$ and n_{ij}^{SC} (t) represent complex Gaussian noise vectors of variance N_0 at the BS i and the SC j in cell i, respectively. The transmit powers of the MUEs and SUEs are denoted by P_{MUE} and P_{SUE}, respectively. Note that the channel vectors are assumed to be constant during each channel coherence block of length T. We assume that the BSs and SCs have perfect knowledge of their local channels, i.e., BS i knows the channel vectors h_{iik}^{BS-MUE} for all k while SC j in cell i knows h_{ijij}^{SC-SUE}. Moreover, both can perfectly estimate their receive covariance matrices for a given coherence block, which are defined as

$$Q_i^{BS} = \mathrm{E}\left[y_i^{BS}(t)\,(y_i^{BS}(t))^H\right] = \sum_{b=1}^{B}\left(\sum_{k=1}^{K} P_{MUE}\, h_{ibk}^{BS-MUE}\,(h_{ibk}^{BS-MUE})^H + \sum_{s=1}^{S} P_{SUE}\, h_{ibs}^{BS-SUE}\,(h_{ibs}^{BS-SUE})^H\right) + NoI_N \tag{3}$$

$$Q_{ij}^{SC} = \mathrm{E}\left(y_{ij}^{SC}(t)\,(y_{ij}^{SC}(t))^H\right) = \sum_{b=1}^{B}\left(\sum_{k=1}^{K} P_{MUE}\, h_{ijbk}^{SC-MUE}\,(h_{ijbk}^{SC-MUE})^H + \sum_{s=1}^{S} P_{SUE}\, h_{ijbs}^{SC-SUE}\,(h_{ijbs}^{SC-SUE})^H\right) + NoI_F. \tag{4}$$

For sufficiently long channel coherence times, these matrices can be well estimated by a simple time average, i.e., $Q_{ij}^{BS} \approx \frac{1}{T}\sum_{t=1}^{T} y_i^{BS}(t)\left(y_i^{BS}(t)\right)^H$ and $Q_{ij}^{SC} \approx \frac{1}{T}\sum_{t=1}^{T} y_{ij}^{SC}(t)\left(y_{ij}^{SC}(t)\right)^H$. We further assume that the noise power N_0 at each receive antenna is explicitly known.

Each individual BS and SC uses its local CSI and its receive covariance matrix to estimate its desired signals via linear minimum mean square error (MMSE) detection, see, e.g., [20]. Under this assumption, the resulting instantaneous UL spectral efficiencies of MUE k and SUE s in cell i are respectively given as

$$R_{ik}^{UL,MUE} = \frac{\mathrm{T_{UL}}}{\mathrm{T}}\log_2\left(1 + SINR_{ik}^{UL,MUE}\right) \tag{5}$$

$$R_{is}^{UL,SUE} = \frac{\mathrm{T_{UL}}}{\mathrm{T}}\log_2\left(1 + SINR_{is}^{UL,SUE}\right) \tag{6}$$

where $\frac{T_{UL}}{T} \in [0,1]$ is the fraction of the coherence time used for UL transmissions. The corresponding signal-to-interference-plus-noise ratios (SINRs) are expressed as

$$SINR_{ik}^{UL,MUE} = P_{MUE}\left(h_{iik}^{BS-MUE}\right)^H \left(Q_i^{BS} - P_{MUE}h_{iik}^{BS-MUE}\left(h_{iik}^{BS-MUE}\right)^H\right)^{-1} h_{iik}^{BS-MUE} \quad (7)$$

$$SINR_{is}^{UL,SUE} = P_{SUE}\left(h_{isis}^{SC-SUE}\right)^H \left(Q_{is}^{SC} - P_{SUE}h_{isis}^{SC-SUE}\left(h_{isis}^{SC-SUE}\right)^H\right)^{-1} h_{isis}^{SC-SUE}. \quad (8)$$

Co-Channel TDD Downlink

During the DL transmissions, the BSs and SCs apply linear precoding to serve their UEs. Hence, the received signals at the *j*th MUE and the *j*th SUE in cell *i* are given as

$$y_{ij}^{MUE}(t) = \sum_{b=1}^{B}\left(\sum_{k=1}^{K}\sqrt{\frac{P_{BS}}{K}}\left(h_{bij}^{BS-MUE}\right)^H w_{bk}^{BS}x_{bk}^{BS}(t) + \sum_{s=1}^{S}\sqrt{P_{SC}}\left(h_{bsij}^{SC-MUE}\right)^H w_{bs}^{SC}x_{bs}^{SC}(t)\right) + n_{ij}^{MUE}(t) \quad (9)$$

$$y_{ij}^{SUE}(t) = \sum_{b=1}^{B}\left(\sum_{k=1}^{K}\sqrt{\frac{P_{BS}}{K}}\left(h_{bij}^{BS-SUE}\right)^H w_{bk}^{BS}x_{bk}^{BS}(t) + \sum_{s=1}^{S}\sqrt{P_{SC}}\left(h_{bsij}^{SC-SUE}\right)^H w_{bs}^{SC}x_{bs}^{SC}(t)\right) + n_{ij}^{SUE}(t) \quad (10)$$

where $x_{bk}^{BS}(t)$ and $x_{bs}^{SC}(t)$ are the complex Gaussian transmitted data symbols from BS *b* to its *k*th MUE and from SC *s* in cell *b* to its SUE, $n_{ij}^{MUE}(t)$ and $n_{ij}^{SUE}(t)$ are noise vectors of variance N_0, and w_{bk}^{BS} and w_{bs}^{SC} are precoding vectors which are respectively defined below (note that these are extensions of the regularized zero-forcing precoder in [27].)

$$w_{bk}^{BS} = \kappa_{bk}^{BS}\left((1-\alpha)\,P_{MUE}\sum_j h_{bbj}^{BS-MUE}\left(h_{bbj}^{BS-MUE}\right)^H + \alpha Q_b^{BS} + (1-\alpha)NoI_N\right)^{-1} h_{bbk}^{BS-MUE} \quad (11)$$

$$w_{bs}^{SC} = \kappa_{bs}^{SC}\left((1-\beta)\,P_{SUE}h_{bsbs}^{SC-SUE}\left(h_{bsbs}^{SC-SUE}\right)^H + \beta Q_{bs}^{SC} + (1-\beta)NoI_F\right)^{-1} h_{bsbs}^{SC-SUE} \quad (12)$$

where $\alpha,\beta \geq 0$ are regularization factors and κ_{bk}^{BS} κ_{bs}^{SC} are normalizing factors, chosen such that $\|w_{bk}^{BS}\|=\|w_{bs}^{SC}\|=1$. The transmit powers of the BSs and SCs are denoted by P_{BS} and P_{SC}, respectively. Note that each BS distributes its transmit power equally among the K MUEs in its cell. The role of the regularization parameters can be explained as follows. For $\alpha,\beta = 0$, the BSs and SCs do not take the interference they may create for neighboring devices into account. Hence, they precode as if they were operating in an isolated cell, i.e., MMSE precoding for the BSs and maximum-ratio transmission for the SCs. On the other hand, large values for the regularization parameters make the precoding vectors more orthogonal to the interference subspace. Thus, by tuning α and β, the BSs and SCs can trade off the beamforming gains for their target UEs against interference reduction to neighboring UEs. Intuitively, a transmitter "sacrifices" some degrees of freedom (or, figuratively speaking, "antennas") to reduce interference towards the directions from which it receives the most interference. Consider a scenario where an MUE is located in the vicinity of an SC. Since the MUE creates strong interference to the SC in the UL, the SC will specifically reduce interference towards this MUE in the DL. Since this precoding technique automatically reduces the negative impact of the strongest sources of interference, one already expects to achieve significant performance gains with few antennas at each SC. This will be demonstrated by simulations in the next section. As such, network-wide TDD and the resulting channel reciprocity allow for cooperation between the devices without any form of data or CSI exchange. This is in stark contrast to network MIMO schemes which require full CSI and user data exchange among multiple BSs or SCs [11]. Moreover, our scheme is fully distributed and scalable. Hence, it is amenable to practical utilizations. Using equation 11 and equation 12, the individual achievable DL rates of MUE *k* and SUE *s* in cell *i* are computed as follows

$$R_{ik}^{DL,MUE} = \left(1 - \frac{T_{UL}}{T}\right)\log_2\left(1 + SINR_{ik}^{DL,MUE}\right) \quad (13)$$

$$R_{is}^{DL,SUE} = \left(1 - \frac{T_{UL}}{T}\right) \log_2 \left(1 + SINR_{is}^{DL,SUE}\right) \quad (14)$$

where the corresponding SINRs are given by

$$SINR_{ik}^{DL,MUE} = \frac{\frac{P_{BS}}{K}\left|\left(h_{iik}^{BS-MUE}\right)^H w_{ik}^{BS}\right|^2}{No + \frac{P_{BS}}{K}\sum_{(b,j)\neq(i,k)}\left|\left(h_{bik}^{BS-MUE}\right)^H w_{bj}^{BS}\right|^2 + P_{SC}\sum_{b,s}\left|\left(h_{bsik}^{SC-MUE}\right)^H w_{bs}^{SC}\right|^2} \quad (15)$$

$$SINR_{is}^{DL,SUE} = \frac{P_{SC}\left|\left(h_{isis}^{SC-SUE}\right)^H w_{is}^{SC}\right|^2}{No + \frac{P_{BS}}{K}\sum_{b,j}\left|\left(h_{bis}^{BS-SUE}\right)^H w_{bj}^{BS}\right|^2 + P_{SC}\sum_{(b,j)\neq(i,s)}\left|\left(h_{bjis}^{SC-SUE}\right)^H w_{bj}^{SC}\right|^2}. \quad (16)$$

Other Duplexing Schemes

Due to their similarity and lack of space, we only briefly summarize the signaling models for the other duplexing schemes. FDD signaling does not create cross-tier interference, but channel reciprocity does not hold either. Therefore, the UL interference covariance matrices cannot be used for DL precoding. Moreover, each tier is assigned only a fraction of the total available bandwidth. We assume that the BSs and SCs apply single-user MMSE detection in the UL and the precoders in equation 11 and equation 12 for $\alpha = \beta = 0$ in the DL. Likewise, the TDD signaling completely nulls the cross-tier interference. However, channel reciprocity holds for each tier and the proposed precoding scheme can be used to reduce intra-tier interference. The interference covariance matrices Q_i^{BS} and Q_{ij}^{SC} are the same as in equation 3 and equation 4, respectively, without the inter-tier interference terms resulting from the transmissions of the MUEs and SUEs. In the coRTDD scheme, both tiers operate on the same band; hence, cross-tier interference plays a major role. The system model is the same as that of the coTDD scheme described earlier, where the only difference is that the order of UL and DL transmissions in the SC tier is reversed. (This also impacts the definition of Q_i^{BS} and Q_{ij}^{SC} in equation 3 and equation 4). In this case, the proposed precoding scheme does not need any modification.

Numerical Results

In this section, we demonstrate the performance of the proposed precoding scheme by numerical simulations. For simplicity, we consider a 3x3 grid of $B = 9$ BSs, where each BS serves $K = 20$ MUEs. Every BS covers an area of one square kilometer (1 km^2) over which $S = 81$ SCs are distributed on a regular grid with an inter-site distance of 111 meters. The MUEs are uniformly randomly distributed over the entire area while one SUE is uniformly distributed within a disc of radius 40 meters around each of the SCs. We ensure that a guard distance of 35 meters from the BSs and 10 meters from the SCs is maintained. The SUEs are associated with their closest SC while the MUEs are associated with their closest BS, even if other cell associations could provide a higher instantaneous rate. This assumption is primarily motivated by a scenario where highly mobile MUEs cannot be associated with SCs due to prohibitive handover signaling. A random snapshot of the center cell is shown in **Figure 4**. We consider a distance-dependent path loss model which encapsulates the effects of small-scale and shadow fading as well as line-of-sight (LOS) and non-LOS (NLOS) links as specified in [1] (Table 6.4-1). The path loss functions, LOS probabilities, and shadowing standard deviations, as well as all other system parameters are summarized in **Table I**. In order to avoid border effects, a wrap-around (torus) topology is assumed so that each macrocell has eight neighboring cells. Note that the SCs, BSs, and all UEs are located outdoors. From the perspective of interference, this is a worst-case scenario since there are no shielding walls separating interfering devices. We compute UL and DL sum rates of the macro and SC tier in the center cell, averaged over 10,000 different channel realizations and UE distributions.

Our baseline scenario is the FDD scheme, assuming that each SC has $F = 1$ and each BS has $N = 20$ antennas. Thus, the number of antennas equals the number of UEs in the system, i.e., the access points need all of their degrees of freedom to serve their UEs. We assume that each tier uses half of its bandwidth for UL and DL transmissions. By changing the fraction of the total bandwidth allocated to each tier,

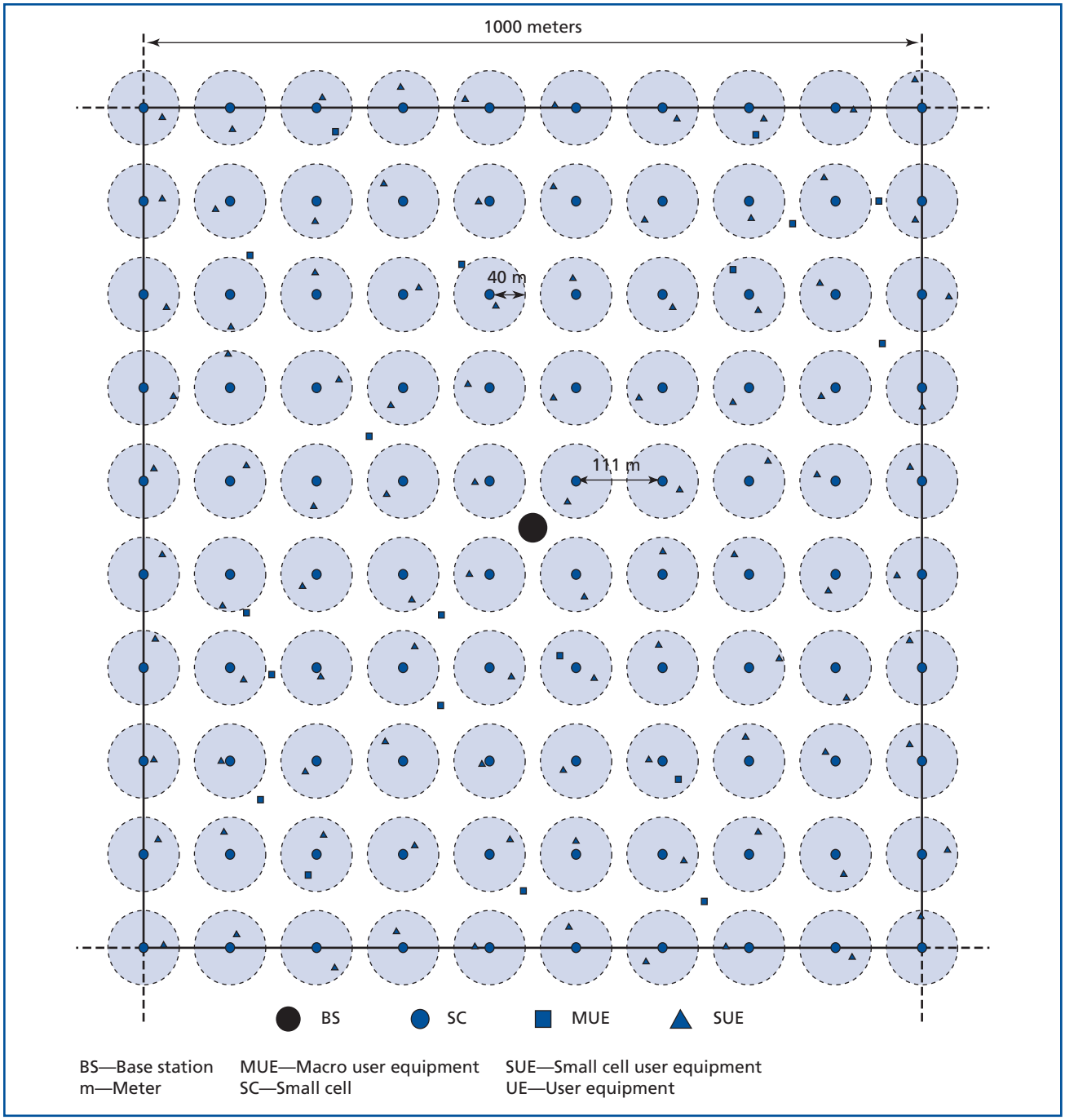

Figure 4.
A random snapshot of the UE distribution in the center macro cell.

we obtain the DL and UL rate-regions as shown by black solid lines in **Figure 5** and **Figure 6**, respectively. Next, with the same duplexing scheme, we demonstrate the gains of having additional antennas in each tier. To this end, each SC is equipped with $F = 4$ and each BS with $N = 100$ antennas, while the number of UEs is kept constant. As can be seen from the dashed lines in Figure 5 and Figure 6, the UL and

Table I. System parameters and path loss models used for simulations.

General system parameters	
Transmit powers	BS: 46 dBm, SC: 24 dBm, MUE/SUE: 23 dBm
Bandwidth	20 MHz, 2 GHz center frequency
Noise power spectral density	−174 dBm/Hz
Network topology	B = 9 macro cells (3x3 regular grid with wrap-around), site distance 1000 m S = 81 small cells per macro cell (regular grid), site distance 111 m
UE deployment	K = 20 MUEs uniformly randomly distributed in each cell 1 SUE uniformly distributed on a disc of radius 40 m around each SC
Antennas	Omnidirectional, N per BS, F per SC, 1 per MUE, 1 per SUE
Propagation parameters	
Channel type	**Path loss and shadowing parameters (d in meters)**
BS – MUE/SUE	$PL_{LOS}(d) = 30.8 + 24.2\log10(d)$ [dB] $PL_{NLOS}(d) = 2.7 + 42.8\log10(d)$ [dB] $Pr_{LOS}(d) = \min(18/d,1)(1-\exp(-d/63))+\exp(-d/63)$ $\Theta_{Shadowing} = 6$ dB
BS – SC	$PL_{LOS}(d) = 30.2 + 23.5\log10(d)$ [dB] $PL_{NLOS}(d) = 16.3 + 36.3\log10(d)$ [dB] $Pr_{LOS}(d) = \min(18/d,1)(1-\exp(-d/72))+\exp(-d/72)$ $\Theta_{Shadowing} = 6$ dB
SC – MUE/SUE	$PL_{LOS}(d) = 41.1 + 20.9\log10(d)$ [dB] $PL_{NLOS}(d) = 32.9 + 37.5\log10(d)$ [dB] $Pr_{LOS}(d) = 0.5\text{-}\min(0.5,5\exp(-156/d))+\min(0.5, 5\exp(-d/30))$ $\Theta_{Shadowing} = 3$ dB (LOS), 4 dB (NLOS)
MUE – SUE	$PL(d) = 38.45 + 20\log10(d)$ [dB], if $d <= 50$ (free space) $PL(d) = 35.78 + 40\log10(d)$ [dB], if $d > 50$ (Xia model) $\Theta_{Shadowing}$: not modeled

BS—Base station
LOS—Line-of-sight
m—Meter
MUE—Macro user equipment
NLOS—Non line-of-sight
PL—Path loss
SC—Small cell
SUE—Small cell user equipment
UE—User equipment

DL rates in both tiers are significantly improved (SC UL + 100 percent, SC DL + 50 percent, macro UL + 200 percent, macro DL + 150 percent). Interestingly, the resulting gains are more pronounced in the UL than in the DL. The reason is that MMSE detection is considered in the UL, which allows for significant interference reduction as the number of antennas grows. However, since channel reciprocity does not hold, the UL covariance matrices cannot be used for DL precoding in order to reduce intra-tier interference. Thus, the gains achievable by adding more antennas are less substantial.

Next, we illustrate the gains from TDD in conjunction with the proposed precoding technique. As before, both tiers operate on different frequency bands, but TDD is used instead of FDD to separate UL and DL transmissions. Since in this case channel reciprocity holds within each tier, the UL covariance information can be used for DL precoding to reduce intra-tier interference. The dashed-and-dotted line in Figure 5 indicates the rate region for the TDD scheme using the precoders as defined in equation 11 and equation 12 with $\alpha = \beta = 1$. Note that the corresponding interference covariance matrices Q_i^{BS} and Q_{ij}^{SC} are defined in equation 3 and equation 4, respectively, without the inter-tier interference terms from the MUEs and SUEs. This leads to an additional DL sum rate gain of about 50 percent in the macro tier and 30 percent in the SC tier. Note that the precoding only affects the DL rates in both tiers. Consequently, the UL rates are the same as in the FDD scheme.

Furthermore, we consider the co-channel deployment of BSs and SCs under the coTDD and coRTDD schemes. In these cases, both tiers use the entire bandwidth and are assumed to assign equal time fractions to UL and DL transmissions, i.e., $\frac{T_{UL}}{T} = 0.5$. This parameter could be changed to further enlarge the rate regions of both duplexing schemes. It is notable that, in the coRTDD scheme, the macro UL and SC DL rates are coupled, i.e., increasing the UL duration of the macro tier decreases the DL duration of the SC tier and vice versa. As before, we assume $N = 100$ and $F = 4$. By tuning the precoding parameters α and β, different points of the rate region can be obtained, as shown by colored trapezoids in Figure 5. Note that the entire rate region has a more complex shape whose characterization is a prohibitive task. The four corner points correspond to the (α,β)-tuples (0,0), (0,1), (1,0), and (1,1). In contrast to TDD, the precoder design now affects the rates of both tiers simultaneously. We focus first on the coTDD scheme. In this case, the DL transmissions of the BSs create significant interference to the SUEs. Hence, increasing α enables the BSs to cancel interference towards the SUEs at the cost of reduced DL rates for their own MUEs. On the other hand, the MUEs experience strong interference from the SCs. Although each SC is equipped with only four antennas, increasing β considerably reduces this interference. As can be seen from Figure 5, the proposed precoding scheme can increase the SC and macro DL sum rates by 50 percent and 200 percent, respectively. Remarkably, the (1,1)-corner point lies well beyond the TDD rate region. This fully justifies the co-channel deployment of SCs and BSs, even in an outdoor scenario with strong interference. The area throughput at this point of the rate region with a 20 MHz bandwidth is 7.63 Gb/s/km^2 (DL) and 8.93 Gb/s/km^2 (UL) which corresponds to an average rate of 38.2 Mb/s (DL) / 25.4 Mb/s (UL) per MUE and 84.8 Mb/s (DL)/104 Mb/s (UL) per SUE.

One can observe that the impact of the precoding scheme is less significant in the coRTDD scheme. The main reason for this is that the interfering links have changed. By increasing α, the BSs can reduce the interference towards the SCs (leading to a 50 percent gain in the SC UL sum rate) at the cost of a reduced SINR for their MUEs (incurring a 40 percent loss in DL sum rate). On the other hand, since the SCs have fewer antennas than the BSs, they cannot reduce cross-tier interference by increasing β. Thus, only the SC DL rates can be improved, by about 15 percent. It is worth highlighting that although coRTDD with the proposed precoding scheme can achieve DL sum rates beyond the TDD rate region, this gain cannot be achieved in the UL.

Discussion

In this section, we discuss implementation considerations along with several practical aspects of the proposed network architecture and precoding scheme, such as channel reciprocity, channel estimation, synchronization, and interference covariance matrix estimation. Furthermore, some advantages of TDD and coRTDD over FDD are explained and possible extensions to FDD and UEs employing multiple antennas are investigated.

Channel Reciprocity

In order to employ the proposed precoding scheme, it is crucial that channel reciprocity holds. Therefore, every UE must be scheduled on the same frequency resources during two subsequent UL and

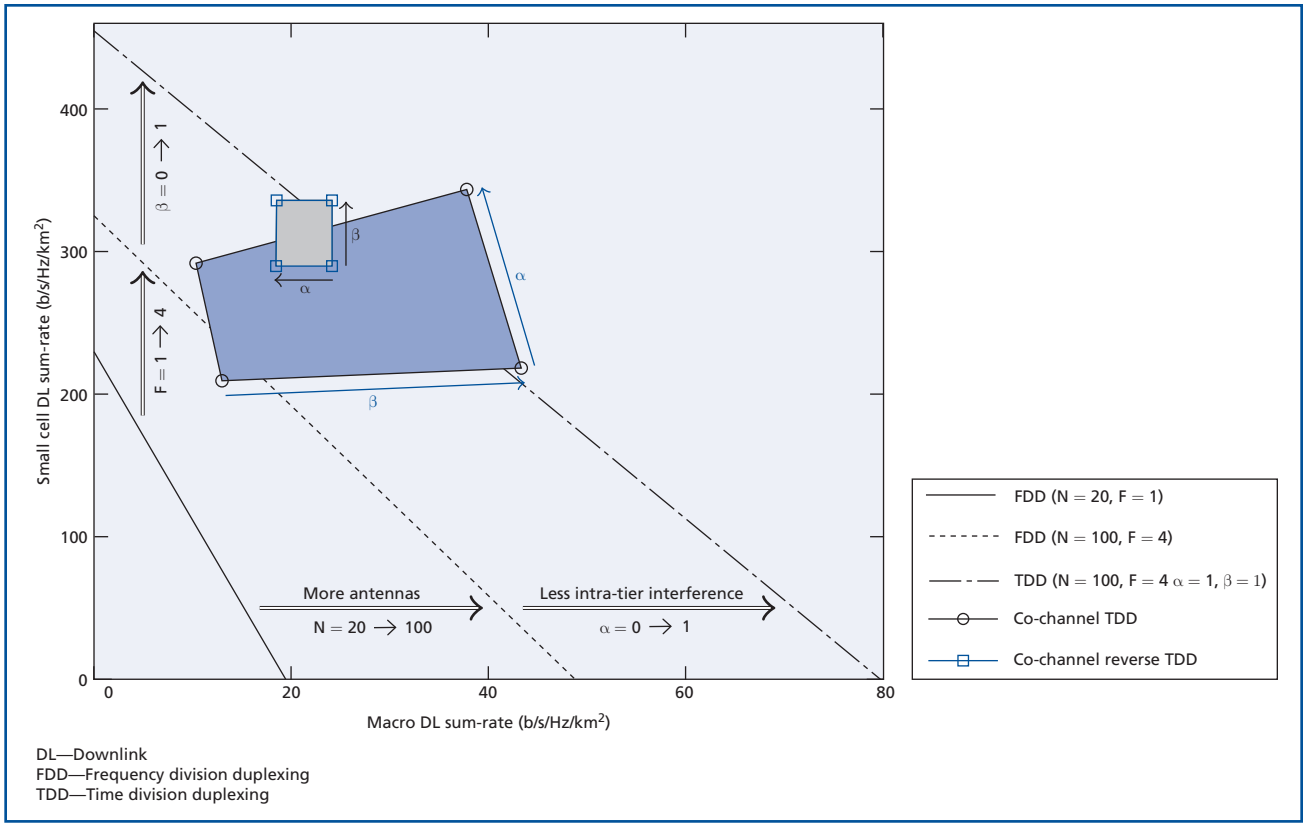

Figure 5.
Macro-small cell downlink rate region with different duplexing schemes.

DL periods. Note that the TDD protocol only ensures the reciprocity of the physical propagation channel. However, in order to achieve full channel reciprocity, one must compensate for random phase and amplitude differences in the transceiver radio frequency (RF) chains [12]. In general, this can be established by either internal self-calibration [13] or external calibration mechanisms [33]. A recent non-commercial testbed developed using off-the-shelf hardware has shown that this is generally possible, even for very large antenna arrays [32]. Nonetheless, even if channel reciprocity holds, the interference levels experienced by the UEs and the access points differ substantially [35]. Thus, some feedback from the UEs for rate adaptation is still necessary. Another important aspect of the network architecture studied in this work is the time synchronization requirement for all devices. Relying on the Global Positioning System (GPS) time information, which today is available at most access points and UEs, this should not be impossible to achieve. Finally, channel reciprocity could be also exploited in FDD systems since the eigenstructure of the wireless channel has been shown to remain similar over a wide range of wavelengths (after appropriate frequency transformation) [14, 17]. The eigenspace of the UL interference covariance matrix could hence be used to design interference-aware precoders similar to the ones proposed in this paper.

Channel Estimation

We have assumed that perfect CSI of the local channels is available at all devices. If channel reciprocity holds, CSI can be acquired at the BSs and SCs from uplink pilots sent by the UEs. In practice, this

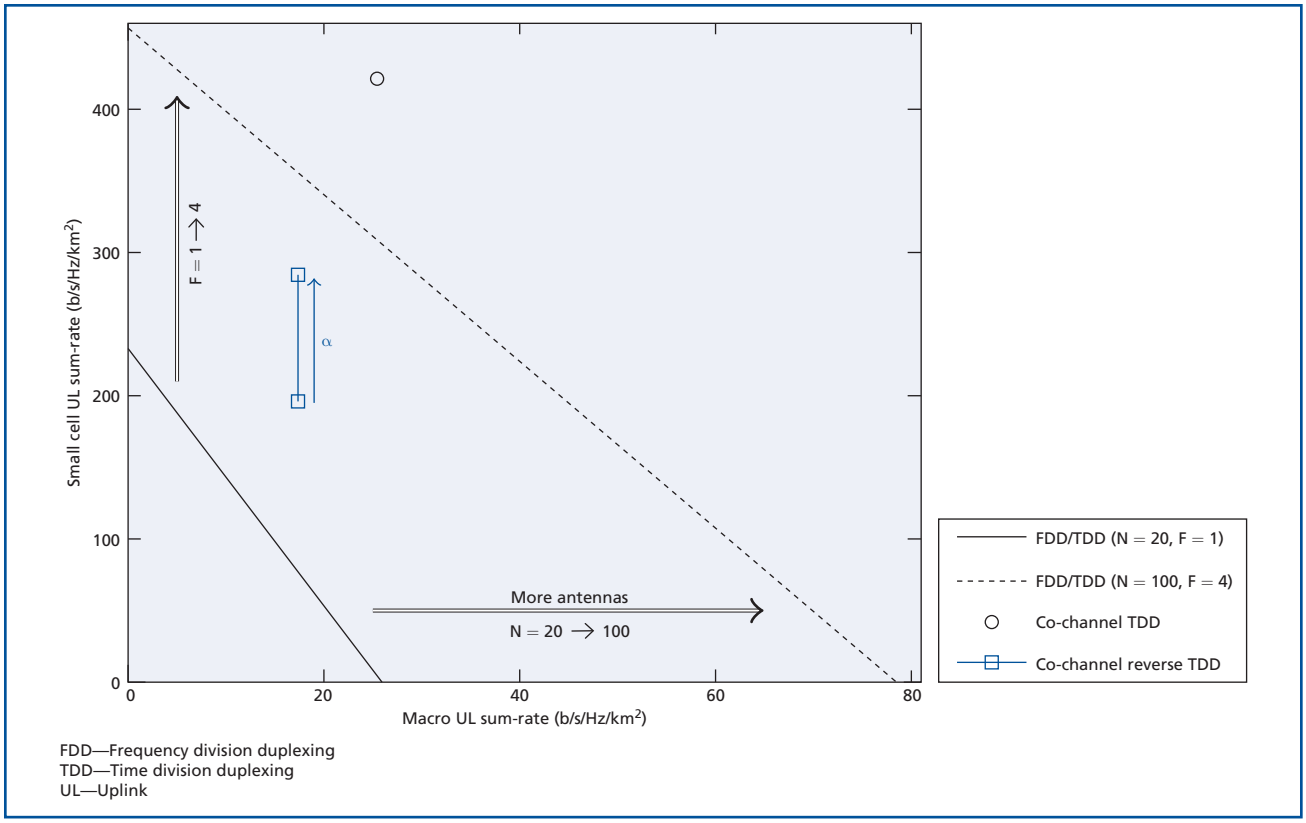

Figure 6.
Macro-small cell uplink rate region with different duplexing schemes.

has currently been exploited only in TDD systems, while FDD systems rely on a combination of downlink training and feedback. Unless certain conditions on the channel eigenstructure are satisfied [3], the overhead for channel training scales linearly with the number of antennas, making the use of very large arrays impossible. Another problem in dense heterogeneous networks is the optimal assignment of pilot sequences to UEs in order to reduce the negative effects of pilot contamination [19, 23]. The co-channel deployment of multiple tiers is expected to render this problem even more difficult. To the best of our current knowledge, this problem has not yet been addressed in the literature.

Estimation of the Interference Covariance Matrix

We have assumed that the BSs and SCs can perfectly estimate their local channels and interference covariance matrices. However, with an increasing number of antennas at the BSs and SCs, this task becomes prohibitive. Classical estimators like the sample covariance matrix which require that the number of antennas is much smaller than the number of observations, i.e., the channel coherence time, fail to work in the large antenna regime [8, 21]. In this context, the coRTDD protocol has the advantage that the interfering channels between the SCs and the BSs are quasi-static so that they could be estimated over very long periods of time.

FDD versus TDD and RTDD

As mentioned earlier, the choice of duplexing mode entails which devices interfere with each other. Apart from that, TDD is not only the key enabler for exploiting channel reciprocity, but it also has several other advantages over FDD which are summarized

here for completeness (see, e.g., [4] for more details). In contrast to FDD, TDD does not require DL feedback of CSI from the UEs, which reduces latency. It further does not need paired frequency bands, which are increasingly difficult to obtain in the overcrowded spectrum. Moreover, TDD can lead to more efficient devices from the perspective of both cost and power since no duplexer is required and the same oscillator and filters are used for UL reception and DL transmissions. Since the entire bandwidth is used, TDD increases the frequency diversity, but also increases the noise power by 3 dB. However, this does not play a major role since dense networks are interference limited. Finally, TDD is more suitable in adapting to asymmetric traffic since the UL/DL ratio can be quickly changed. As mentioned earlier, since the MUEs are prone to strong interference from the SC tier, DL in the macrocell is considered to be the main performance bottleneck. Reducing this interference is thus of utmost importance. In this regard, coRTDD is a less promising candidate than coTDD since only BS-to-SC interference can be reduced.

Possible Extensions

First, our proposed scheme could be extended to the case of multi-antenna UEs in a rather straightforward manner. This would enable the UEs to estimate their interference covariance matrices and employ precoders to reduce interference to adjacent access points or UEs during the UL transmissions. Second, we have considered a worst-case scenario without any form of power control, cell association, and user scheduling. By employing location-dependent user scheduling and interference-temperature power control schemes, the network-wide performance could be further enhanced [2]. Third, more sophisticated duplexing schemes could be considered. For example, an attractive alternative to coTDD is band switching duplexing [6] (see also [4]). In this scheme, both tiers operate simultaneously on two frequency bands over which they apply TDD in reversed orders. Thus, every device is permanently in UL and DL mode so that conventional TDD-duplexing delays are reduced. One could further reverse the orders of UL and DL for certain fractions of devices in the network to favorably shape the interference distribution.

Summary and Conclusions

In this paper, we have presented a TDD-based network architecture which integrates the complementary benefits of a massive MIMO macro tier overlaid with a dense tier of SCs. The synchronized network-wide TDD protocol is the key enabler for exploiting channel reciprocity which allows every device to reuse its received interference covariance matrix estimate for interference-aware precoding. Based on this observation, we have proposed a simple precoding scheme which relies only on local information, does not require any data exchange between the devices, and is hence fully distributed and scalable. Simulation results have shown that this architecture can achieve an area throughput on the order of tens of Gb/s per square kilometer, which can be further improved by either installing more BS antennas or deploying more SCs. In summary, we believe that a TDD-based heterogeneous network architecture consisting of massive MIMO BSs and SCs is a very attractive candidate for the next generation of cellular networks.

Acknowledgements

Kianoush Hosseini was supported by the PhD@Bell Labs internship program. Parts of this work have been performed in the framework of the FP7 project ICT-317669 METIS.

References

[1] 3rd Generation Partnership Project, "Technical Specification Group Radio Access Network, Evolved Universal Terrestrial Radio Access (E-UTRA), Further Enhancements to LTE Time Division Duplex (TDD) for Downlink-Uplink (DL-UL) Interference Management and Traffic Adaptation (Release 11)," 3GPP TR 36.828, v11.0.0, June 2012, <http://www.3gpp.org/ftp/Specs/html-info/36828.htm>.

[2] A. Adhikary and G. Caire, "On the Coexistence of Macrocell Spatial Multiplexing and Cognitive Femtocells," Proc. IEEE Internat. Conf. on Commun. (ICC '12), SmallNets: 1st Internat. Workshop on Small Cell Wireless Networks (ICC '12 WS) (Ottawa, Ont., Can., 2012), pp. 6830–6834.

[3] A. Adhikary, J. Nam, J.-Y. Ahn, and G. Caire, "Joint Spatial Division and Multiplexing," arXiv:1209.1402v2, Jan. 2013, <http://arxiv.org/abs/1209.1402>.

[4] A. Alexiou, D. Avidor, P. Bosch, S. Das, P. Gupta, B. Hochwald, T. E. Klein, J. Ling, A. Lozano, T. L. Marzetta, S. Mukherjee, S. Mullender, C. B. Papadias, R. A. Valenzuela, and H. Viswanathan, "Duplexing, Resource Allocation and Inter-Cell Coordination: Design Recommendations for Next Generation Wireless Systems," Wireless Commun. and Mobile Comput., 5:1 (2005), 77–93.

[5] J. G. Andrews, H. Claussen, M. Dohler, S. Rangan, and M. C. Reed, "Femtocells: Past, Present, and Future," IEEE J. Select. Areas Commun., 30:3 (2012), 497–508.

[6] P. Bosch and S. J. Mullender, "Band Switching for Coherent Beam Forming in Full-Duplex Wireless Communication," U.S. Patent 2005/0243748 A1 (2005).

[7] H. Claussen, "Co-Channel Operation of Macro- and Femtocells in a Hierarchical Cell Structure," Internat. J. Wireless Inform. Networks, 15:3–4 (2008), 137–147.

[8] R. Couillet and M. Debbah, "Signal Processing in Large Systems: A New Paradigm," IEEE Signal Process. Mag., 30:1 (2013), 24–39.

[9] F. Fernandes, A. Ashikhmin, and T. L. Marzetta, "Interference Reduction on Cellular Networks with Large Antenna Arrays," Proc. IEEE Internat. Conf. on Commun. (ICC '12) (Ottawa, Ont., Can., 2012), WC14: Space-Time Coding II.

[10] G. J. Foschini and M. J. Gans, "On Limits of Wireless Communications in a Fading Environment When Using Multiple Antennas," Wireless Personal Commun., 6:3 (1998), 311–335.

[11] D. Gesbert, S. Hanly, H. Huang, S. Shamai Shitz, O. Simeone, and W. Yu, "Multi-Cell MIMO Cooperative Networks: A New Look at Interference," IEEE J. Select. Areas Commun., 28:9 (2010), 1380–1408.

[12] J.-C. Guey and L. D. Larsson, "Modeling and Evaluation of MIMO Systems Exploiting Channel Reciprocity in TDD Mode," Proc. 60th IEEE Veh. Technol. Conf. (VTC '04–Fall) (Los Angeles, CA, 2004), vol. 6, pp. 4265–4269.

[13] M. Guillaud, D. T. M. Slock, and R. Knopp, "A Practical Method for Wireless Channel Reciprocity Exploitation Through Relative Calibration," Proc. 8th Internat. Symp. on Signal Process. and Its Applications (ISSPA '05) (Sydney, Aus., 2005), pp. 403–406.

[14] B. M. Hochwald and T. L. Marzetta, "Adapting a Downlink Array from Uplink Measurements," IEEE Trans. Signal Process., 49:3 (2001), 642–653.

[15] J. Hoydis, M. Kobayashi, and M. Debbah, "Green Small-Cell Networks: A Cost- and Energy-Efficient Way of Meeting the Future Traffic Demands," IEEE Veh. Technol. Mag., 6:1 (2011), 37–43.

[16] H. Huang, C. B. Papadias, and S. Venkatesan, MIMO Communication for Cellular Networks, Springer, New York, 2012, Chapter 6.3.2.

[17] K. Hugl, K. Kalliola, and J. Laurila, "Spatial Reciprocity of Uplink and Downlink Radio Channels in FDD Systems," COST 273 TD(02) 066, May 2002, <http://publik.tuwien.ac.at/files/pub-et_10343.pdf>.

[18] Institute of Electrical and Electronics Engineers, "Part 11: Wireless LAN Medium Access Control (MAC) and Physical Layer (PHY) Specifications, Amendment 5: Enhancements for Higher Throughput," IEEE 802.11n-2009, Sept. 2009.

[19] J. Jose, A. Ashikhmin, T. L. Marzetta, and S. Vishwanath, "Pilot Contamination and Precoding in Multi-Cell TDD Systems," IEEE Trans. Wireless Commun., 10:8 (2011), 2640–2651.

[20] S. M. Kay, Fundamentals of Statistical Signal Processing: Estimation Theory, Prentice-Hall, Upper Saddle River, NJ, 1993, Chapter 14.2.

[21] O. Ledoit and M. Wolf, "A Well-Conditioned Estimator for Large-Dimensional Covariance Matrices," J. Multivariate Anal., 88:2 (2004), 365–411.

[22] B. O. Lee, H. W. Je, I. Sohn, O.-S. Shin, and K. B. Lee, "Interference-Aware Decentralized Precoding for Multicell MIMO TDD Systems," Proc. IEEE Global Telecommun. Conf. (GLOBECOM '08) (New Orleans, LA, 2008).

[23] T. L. Marzetta, "Noncooperative Cellular Wireless with Unlimited Numbers of Base Station Antennas," IEEE Trans. Wireless Commun., 9:11 (2010), 3590–3600.

[24] F. Negro, I. Ghauri, and D. T. M. Slock, "Beamforming for the Underlay Cognitive MISO Interference Channel via UL-DL Duality," Proc. 5th Internat. Conf. on

Cognitive Radio Oriented Wireless Networks and Commun. (CrownCom '10) (Cannes, Fra., 2010).
[25] H. Q. Ngo, E. G. Larsson, and T. L. Marzetta, "Energy and Spectral Efficiency of Very Large Multiuser MIMO Systems," IEEE Trans. Commun., 61:4 (2013), 1436–1449.
[26] H. Q. Ngo, T. L. Marzetta, and E. G. Larsson, "Analysis of the Pilot Contamination Effect in Very Large Multicell Multiuser MIMO Systems for Physical Channel Models," Proc. IEEE Internat. Conf. on Acoustics, Speech, and Signal Process. (ICASSP '11) (Prague, Cze. Rep., 2011), pp. 3464–3467.
[27] C. B. Peel, B. M. Hochwald, and A. L. Swindlehurst, "A Vector-Perturbation Technique for Near-Capacity Multiantenna Multiuser Communication—Part 1: Channel Inversion and Regularization," IEEE Trans. Commun., 53:1 (2005), 195–202.
[28] Qualcomm, "The 1000x Data Challenge," <http://www.qualcomm.com/1000x/>.
[29] S. Rangan, "Femto-Macro Cellular Interference Control with Subband Scheduling and Interference Cancelation," Proc. IEEE GLOBECOM Workshops (GC Wkshps '10) (Miami, FL, 2010), Workshop on Interference Management for Femtocell Networks, pp. 695–700.
[30] F. Richter, G. Fettweis, M. Gruber, and O. Blume, "Micro Base Stations in Load Constrained Cellular Mobile Radio Networks," Proc. 21st IEEE Internat. Symp. on Personal, Indoor and Mobile Radio Commun. Workshops (PIMRC '10 WS) (Istanbul, Tur., 2010), pp. 357–362.
[31] F. Rusek, D. Persson, B. K. Lau, E. G. Larsson, T. L. Marzetta, O. Edfors, and F. Tufvesson, "Scaling Up MIMO: Opportunities and Challenges with Very Large Arrays," IEEE Signal Process. Mag., 30:1 (2013), 40–60.
[32] C. Shepard, H. Yu, N. Anand, L. E. Li, T. Marzetta, R. Yang, and L. Zhong, "Argos: Practical Many-Antenna Base Stations," Proc. 18th Annual Internat. Conf. on Mobile Comput. and Networking (MobiCom '12) (Istanbul, Tur., 2012), pp. 53–64.
[33] J. Shi, Q. Luo, and M. You, "An Efficient Method for Enhancing TDD over the Air Reciprocity Calibration," Proc. IEEE Wireless Commun. and Networking Conf. (WCNC '11) (Cancun, Mex., 2011), pp. 339–344.
[34] E. Telatar, "Capacity of Multi-Antenna Gaussian Channels," Eur. Trans. Telecommun., 10:6 (1999), 585–595.
[35] A. Tölli and M. Codreanu, "Compensation of Interference Non-Reciprocity in Adaptive TDD MIMO-OFDM Systems," Proc. 15th IEEE Internat. Symp. on Personal, Indoor and Mobile Radio Commun. (PIMRC '04) (Barcelona, Spn., 2004), vol. 2, pp. 859–863.
[36] W. Webb, Wireless Communications: The Future, John Wiley & Sons, Hoboken, NJ, 2007, Chapter 6.3.4.
[37] P. Xia, V. Chandrasekhar, and J. G. Andrews, "Open vs. Closed Access Femtocells in the Uplink," IEEE Trans. Wireless Commun., 9:12 (2010), 3798–3809.
[38] R. Zhang, F. Gao, and Y.-C. Liang, "Cognitive Beamforming Made Practical: Effective Interference Channel and Learning-Throughput Tradeoff," IEEE Trans. Commun., 58:2 (2010), 706–718.

(Manuscript approved March 2013)

JAKOB HOYDIS is a member of technical staff in the Wireless Physical Layer Research Department at Bell Labs in Stuttgart, Germany. He received his diploma degree (Dipl.-Ing.) in electrical engineering and information technology from RWTH Aachen University, Germany, and his Ph.D. degree from Supélec, Gif-sur-Yvette, France. His research interests are in the areas of large random matrix theory, information theory, signal processing, and wireless communications. Dr. Hoydis was awarded the 2012 Supélec Publication Prize for his dissertation.

KIANOUSH HOSSEINI was an intern with the Wireless Physical Layer Research Department at Bell Labs in Stuttgart, Germany, during the summer of 2012. He received his B.Sc. degree in electrical engineering from Iran University of Science and Technology, Tehran, Iran, and his M.A.Sc. degree in electrical and computer engineering from the University of Toronto, Toronto, Ontario, Canada. He is currently pursuing a Ph.D. degree in electrical and computer engineering at the University of Toronto. His main research interests include signal processing, optimization, distributed algorithms, and their applications in wireless communications.

STEPHAN TEN BRINK is the head of the Wireless Physical Layer Research Department at Bell Labs in Stuttgart, Germany. He received a Dipl.-Ing. and a Dr.-Ing. degree in electrical engineering, both from the University of Stuttgart, Germany. He spent the first five years of his career at Bell Labs' Wireless Research Laboratory in Holmdel, New Jersey, conducting research on channel coding for multiple antenna systems, and later moved to Realtek Semiconductor Corporation in Irvine, California, where he spent seven years developing application-specific integrated circuit (ASIC) solutions for wireless local area network (LAN) and ultra-wideband systems. He returned to Bell Labs three years ago to head the Wireless Physical Layer Research department. Dr. ten Brink is a recipient of several awards, including the Vodafone Innovation Award in 2003 and the IEEE Stephen O. Rice prize in 2005 for contributions to channel coding and signal detection. His research interests include multiple-antenna communications and channel coding for wireless and optical systems.

MÉROUANE DEBBAH is the head of the Alcatel-Lucent Chair on Flexible Radio at Supélec, Gif-sur-Yvette, France. He received M.Sc. and Ph.D. degrees from the Ecole Normale Supérieure de Cachan (France). Earlier in his career, he worked for Motorola Labs on wireless local area networks and prospective fourth generation systems, and as a senior researcher at the Vienna Research Center for Telecommunications (FTW) Vienna, Austria. He also served as an assistant professor in the Mobile Communications department of the Institut Eurecom, Sophia Antipolis, France. His research interests are in information theory, signal processing, and wireless communications. Dr. Debbah received the Mario Boella prize in 2005, the 2007 General Symposium IEEE GLOBECOM best paper award, the Wi-Opt 2009 best paper award, the 2010 Newcom++ best paper award, as well as the Valuetools 2007, Valuetools 2008, and CrownCom 2009 best student paper awards. He is a WWRF fellow. In 2011, he received the IEEE Glavieux Prize Award. He is the co-founder of the Live Video Network Ximinds (http://www.ximinds.com). ◆